



Additive surface texturing of cutting tools using pulsed laser implantation with hard ceramic particles

S. Böhm¹ · A. Ahsan¹ · J. Kröger¹ · J. Witte¹

Received: 5 June 2020 / Accepted: 6 September 2020 / Published online: 15 September 2020
© The Author(s) 2020

Abstract

In recent years surface texturing of the cutting tools has proved to improve tribological characteristics at tool/chip and tool/workpiece interface and help to reduce cutting and feed forces as well as tool wear. Most, if not all, of the studies have focused on subtractively made textures whereby the material is removed from the surface. This study investigates the performance of additively made surface structures whereby hard ceramic particles are dispersed in the form of dome shaped textures on the surface of the cutting tools using solid state millisecond pulsed laser (pulsed laser implantation). Dry cutting tests were performed on ductile cast iron. The results show a greater reduction of process forces with implantation of flank face as compared to rake face. Both cutting and feed forces were reduced by 10% compared to the non-structured tool. In addition, the tool life increased by a factor of 3 whereas the average flank wear reduced by as much as 80% and cutting edge rounding by up to 60%.

Keywords Cutting tool · Surface texturing · Laser dispersing · Laser implantation · Surface structuring

1 Introduction

In machining processes, the cutting tools are required to possess high surface hardness to slow down abrasive wear rate, good fracture toughness to avoid edge chipping and cracking, thermal stability at cutting temperatures as well as low chemical affinity with the work material. In addition, low friction coefficient is required between the tool and the work material to minimize resistance to material flow and

overheating at the tool/chip and tool/workpiece interfaces [2, 4]. Thus, minimization of friction during cutting leads to greater tool life, improved surface quality, higher cutting speeds and increased productivity. The industrial practice to improve tribological characteristics includes low-friction coatings [5, 12, 13, 20, 23] and novel lubrication techniques [3, 29, 31, 36].

1.1 Surface texturing by material removal

Surface texturing has been shown to be an effective method for improving the tribological behaviour under both full-film as well as boundary lubrication conditions for various applications [9, 14]. Advances in ultrashort pulsed lasers (pulse duration times in pico- and femtosecond regions) has led to numerous research studies on the effect of surface texturing of cutting tools on machining performance and tool life. Fatima et al. [10] produced grooves on both rake and flank face of uncoated carbide turning insert using femtosecond laser for cutting AISI4140 steel with a lubricant. They reported a reduction of friction coefficient, cutting force and feed force of 18%, 10% and 23% respectively. Fatima et al. [11] also carried out tests with micro-grooves on only the flank face of carbide tips and reported reduction in process forces and cutting power of 12% and 37%

This project (HA Project No. 695/19-15) is funded in the framework of Hessen Modellprojekte, financed with funds of LOEWE – Landes-Offensive zur Entwicklung Wissenschaftlich-ökonomischer Exzellenz, Förderlinie 3: KMU-Verbundvorhaben (State Offensive for the Development of Scientific and Economic Excellence)

✉ A. Ahsan
a.ahsan@uni-kassel.de

S. Böhm
s.boehm@uni-kassel.de

J. Kröger
j.kroeger@uni-kassel.de

¹ Department of Cutting and Joining Technology (tff),
University of Kassel, Kurt-Wolters-Str. 3, 34125 Kassel,
Germany

respectively. They also reported an 18% increase in tool life. Thomas et al. [19] created dimples on high speed steel lathe tool and performed dry cutting of an aluminium alloy and mild steel. They reported a cutting force reduction of 41% for aluminium and 20% for mild steel when using textured tools. In addition, cutting temperature was reduced by 3% and 13% for aluminium and mild steel, respectively.

In their study of turning aluminium alloy A5052 with micro and nanotextured uncoated tungsten carbide tools under minimum quantity lubrication, Kawasegi et al. [21] created grooves perpendicular and parallel to the main cutting edge on rake face. They reported a greater change in feed and thrust force as compared to the cutting force with micro-grooves on the rake face. However, only a minor reduction of forces was observed with nano-textures compared to micro-textures. In a similar study Kiyota et al. [22] used femtosecond laser to create dimples and grooves of 20 μm diameter (width) and 10 μm depth on uncoated carbide tools for dry orthogonal cutting of AISI1045 steel. They report only a 10% reduction in forces and around 15% reduction in coefficient of friction but only at speeds above 150 m/min. It was also concluded that textures on the rake face lead to greater built up material which however causes reduction of tool/chip contact area. Enomoto et al. [7, 8] performed milling experiments with a tungsten carbide tool having nano-/micro-textures on the rake face. The nano-textures did not improve wear characteristics whereas micro-stripe textures significantly reduced crater-wear. The friction coefficient was reduced by about 10%. The authors also CVD coated the textured tools with TiAlN which further reduced wear and chip adhesion. Yamaguchi et al. [35] performed pin-on-disc tests with electrical discharge textured steel disc to determine the effect of micro-textures under lubrication and reported a reduction of coefficient of friction of up to 40%. Xing et al. [34] used nanosecond laser to create micro-textures on the rake face and nano-textures on chamfer of the carbide tool in turning experiments of hardened (50 HRC) 1045 steel. They reported a reduction in cutting force of about 15–20% and in radial thrust force of 30–35% and a reduction in cutting temperature of about 20%. However, the surface roughness of the machined workpieces was higher for the textured tools. Similar results were also reported by Denkena et al. [6] and Li et al. [24] for PcBN tools. In their recent publication, Ahmed et al. [1] reported reductions of 58%, 100% and 24% respectively for cutting force, axial force and friction coefficient with femtosecond laser ablated square textures on the rake face of carbide tool when turning AISI304 stainless steel.

1.2 Surface texturing by material addition

One common feature among the above mentioned studies is the use of the subtractive texturing methods whereby the

material is removed from the surface. On the other hand, additive surface texturing, to the best of authors' knowledge, has not been explored on cutting tools. Additive surface modification methods using lasers include laser cladding, laser surface alloying and laser dispersion [18]. One of the most recent developments in surface modification using laser is the so called 'pulsed laser implantation' (hereafter abbreviated as PLI). A variant of laser dispersion, it combines the effect of surface texturing with optimization of surface material. First developed by Steinhoff and Schulheit et al. [26, 28] at the University of Kassel, Germany for wear reduction of cold forging tools, the process uses a pulsed laser with longer pulse durations (millisecond range) on the target material covered with thin bed of hard ceramic powders. The energy transfers through the powder bed and melts the substrate in small spots causing the ceramic particles to disperse in the melt pool (see Fig. 1). The material added to the melt forms dome-shaped dispersion hardened implants which are raised in relation to the substrate surface. Finally, the remaining precoating is cleaned from the surface. The contact surface to the workpiece is reduced to the wear-resistant implants, thus protecting the base material [16].

The properties such as dimension and hardness of these surface structures can be specifically controlled by influencing variables such as the type of hard material, particle size and especially by varying the laser parameters. The controllability and variety of the laser implantation process makes the method attractive for applications with complex contours and tribological challenges. The process of PLI differs from traditional coating processes in that it provides a harder and wear resistant surface in specific (dome shaped) textures instead of a smooth continuous layer. This causes a reduction in contact area at the chip/tool (rake face) and workpiece/tool (flank face) interfaces and thus helps to reduce friction and heat generation. The resulting micro-dome is a dispersion hardened material and not a uniform material (like a coating) and therefore lacks the hardness and thermal properties of a coating. However, the presence of harder surface textures in relation to the base material helps improve

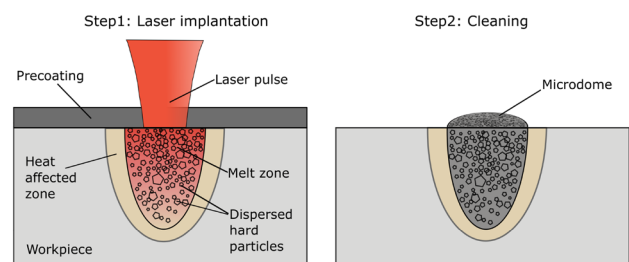


Fig. 1 Processing steps for laser implantation with the laser pulse directed on to the workpiece with precoating of hard particles and binder along with the melt and heat affected zones (left) and the resulting micro-dome with dispersed hard particles (right)

the wear resistance and tribological performance. Hilgenberg et al. [17] used TiB₂, TiC and WC particles for laser implantation of X153CrMoV12 steel for cold rolling rolls. They reported higher hardness of the implants at lower pulse intensities and onset of the keyhole effect at higher intensities. Maximum hardness values in the implanted zones for TiB₂, TiC and WC particles were found to be 1600 HV (Vicker’s hardness), 1250 HV and 1100 HV respectively. Spranger et al. [27] reported a dispersion fraction of 40–55% for TiB₂ particles in the laser implanted zone and hardness values as high as 1800 HV. In their study of friction stir welding pins implanted with boron carbide (B₄C) particles, Schuedekopf et al. [25] reported an increase in the tool life of up to 70%.

This novel surface texturing method offers a promising perspective especially for high speed steel (HSS) special tools such as band saws or hobs, where an economical coating is often not possible. In addition, there are potentials for energy saving through friction reduction due to the positive tribological properties of the implants [35]. Therefore, it is the aim of this paper to investigate the effect of PLI of hard particles on the performance of HSS tools in dry orthogonal cutting experiments. PLI of cutting tools is primarily intended for reducing wear of the tools in roughing operations. The laser implanted structures, specially on the flank face, would result in smaller but multiple contacts resulting in higher surface roughness than non-implanted tools and therefore not suitable for finishing operations.

2 Materials and methods

For this investigation HSS type DIN HS6-5-2-10 (C: 0.85%; W: 6.5%; Mo: 5%; V: 2%; Co: 10%) was used as the tool material. The hardness of the material in as delivered state was 1060 HV (67 HRC). The tool geometry, shown in Fig. 2, was wire-eroded and ground to a form similar to a saw tip. The tool had a width of 1.8 mm and +5° rake and relief angles. The rake and flank face were both ground to a surface roughness Rz 3 μm and a cutting edge radius of 10 μm. Surface roughness was measured using optical profilometer

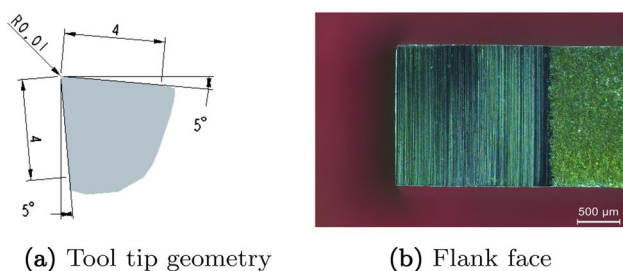


Fig. 2 High speed steel tool geometry used in the cutting tests

of manufacturer FRT GmbH and the edge radius was measured using light fringe projection profilometer of manufacturer LMI Technologies. The side relief angle was not ground on the tool.

2.1 Laser implantation

Pulsed laser implantation was performed using an Nd:YAG pulsed fiber laser of type LASAG KLS-246-C having a wavelength of 1064 nm, pulse duration 0.1–20 ms, pulse frequency 0.1–500 Hz, average pulse power 10–220 W, peak power 5.5 kW and peak energy 50 J. The parameter study for laser implantation was performed on flat samples of HS6-5-2-10 having a thickness of 3 mm. Tungsten carbide (WC) particles were used for pulsed laser implantation. The physical properties of the powder are given in Table 1.

The precoat of hard particles was applied as a slurry containing 75 wt% hard particles, 20 wt% organic binder (polyvinyl butyral (PVB)) and 5 wt% ethanol using an air-brush gun. Three precoat thicknesses were applied i.e. 75 μm, 150 μm and 300 μm. The thickness of the precoat was measured non-destructively using a calibrated eddy current sensor. The precoated samples were allowed to dry and harden at room temperature for 24 h after which the precoat was ready for laser implantation. After precoating with different thicknesses, PLI was performed by varying pulse power Pp, pulse length tp as well as distance from focus Δf (see Table 2). The focus distance has an influence on the spot diameter and thus also on the area intensity of the laser

Table 1 Properties of WC particles at 20°C used for pulsed laser implantation [15]

Property	Value
Hardness	2400 HV1
Particle size	1 μm
Melting point	2780 °C
Elasticity module	550 GPa
Thermal expansion coefficient	4.9 × 10 ⁻⁶ K ⁻¹
Density	15.8 g/cm ³
Thermal conductivity	117 Wm ⁻¹ K ⁻¹

Table 2 Experimental plan for parameter study of laser implantation of flat HSS samples with variation of precoat thickness, pulse length, distance from focus and average laser power

Factors	Levels
Precoat thickness [μm]	75; 150; 300
Average laser power [W]	50; 100; 150
Pulse duration [ms]	1; 2; 3; 4; 5
Distance from focus [mm]	0; 1

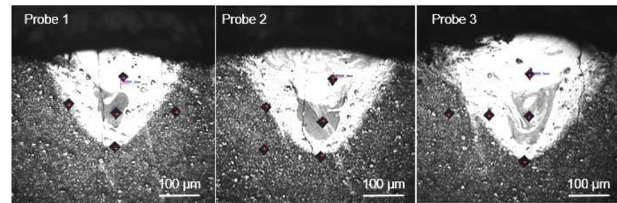
Table 3 Selected parameters for laser implantation

Parameter	Value
Coat thickness	150 μm
Pulse power	100 W
Pulse duration	4 ms
Focus distance	0 mm
Focus radius	88 μm
Pulse energy	437 mJ
Laser intensity	450 kW/cm^2

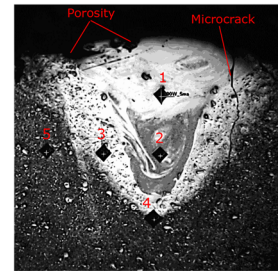
beam and is set to $\Delta f = 0$ mm and 1 mm. A positive value of the focus position means that the focus point is above the substrate surface, a negative value means that the focus is below the surface.

For each parameter combination a single sample with 23 spots placed 500 μm away from each other and with a 50 μm offset between adjacent rows of spots was prepared. The offset increases the probability of cutting through the middle of the implant for microscopy and hardness measurements. For the identification of optimal parameters, the penetration of the implant zones, the shape of the domes, the height above the substrate, diameter of the spots as well as the microstructural defects such as pores, micro-cracks and keyhole effect were used as the selection criterions. From a detailed parameter study, which is not the subject of this paper, the parameter combination given in Table 3 was selected. The laser implantation of HSS samples with selected parameters result in an average spot diameter of 200 μm and height of the domes above the surface of about 20 μm . Figure 3 shows the melt zone as well as the heat affected zone (HAZ) in the cross section of the implanted region. The HAZ appears to be less than 100 μm which is 400 μm less than the distance between each spot (distance between closest edges). Therefore, the residual heating effect from one spot to the next could be neglected.

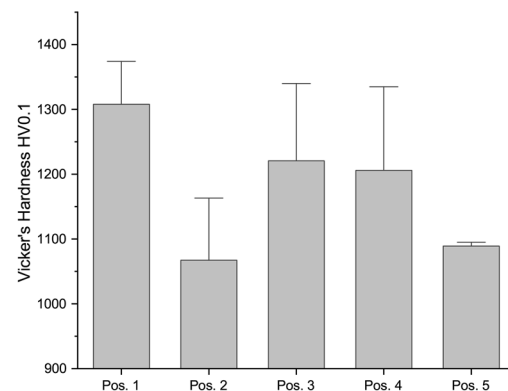
For the microhardness measurement in the cross-section of the implantation, a total of nine spots were created on a flat high speed steel sample. After implantation the sample was then wire eroded such that multiple implantation spots are cut through the center. The cross-sections were then embedded in epoxy resin, ground, polished and etched with 5 % Nital solution for 30 seconds to enhance the microstructures. Cross-sections of the three of the nine implantation spots are shown in Fig. 3a. The hardness was then measured in five regions in the cross section using Micro Vickers test apparatus with 0.1 kg load (see Fig. 3b). Bright appearance of the region 1 indicate a higher dispersion of WC particles and a hardness increase of about 20 % compared to the base material was observed for this region (see Fig. 3c). This is also where the highest hardness is desired to resist abrasive wear. In the dark appearing core area (region 2) the dispersion is less, so that a lower hardness was observed.



(a) Cross section of three implanted spots 1, 2 and 3 with indentation marks for hardness measurements in five different regions of the cross-section.



(b) Cross-section of the sample 3 with hardness measurement indentations marked in red as numbers 1 through 5.



(c) Microhardness of five regions in the cross section of implanted spots labeled in Fig. 3b ($N = 9$).

Fig. 3 Micro-hardness measurement of the implanted spots ($N = 9$)

The heat-affected region (region 3) and the transition region (region 4) were also hardened with respect to the base material (region 5). Scanning electron microscopy (SEM) and Energy Dispersive X-Ray Analysis (EDX) were not available for this study. However, implantation with tungsten carbide particles of 10 μm average size was performed at the tff institute of the university of Kassel by [32] for friction stir welding tool made of tool steel 1.2343 and SEM / EDX analysis was performed. Figure 4 shows the backscattered electron image and the EDX analysis of distribution of tungsten (W) in the implanted region. The precoating thickness hereby was also 150 μm , average pulse power 80 W and pulse duration was 5 ms. The EDX analysis shows that similar to the observation in Fig. 3, two distinct regions in

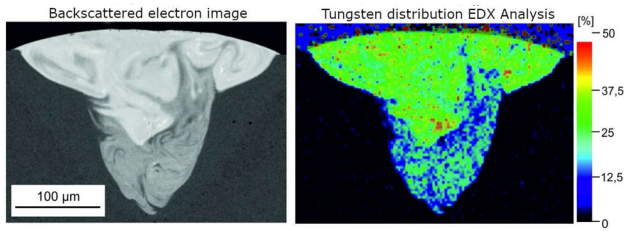


Fig. 4 Distribution of tungsten in the laser implanted zone on tool steel 1.2343 using tungsten carbide particles [32]

the implanted zones are present. The upper portion contains around 30–40% WC particles by volume while the lower region about 15%. The EDX results also show that some of the WC particles melt and are finely distributed in the matrix.

2.2 Orthogonal cutting tests

After the selection of the optimum parameter combination, PLI of the HSS cutting tool (see Fig. 2) was performed. Four variations of the tool were evaluated including a non-implanted tool (shown in Fig. 2b), tool with implanted rake face (SF), implanted flank face (FF) and one variant where both rake and flank face were implanted (SF+FF) with tungsten carbide particles (see Fig. 5). For all implanted variants, PLI was performed in a 6 x 6 spot raster with each spot having a diameter of approximately 200 μm and a protrusion above the surface of about 20 μm. The outer edge of the first

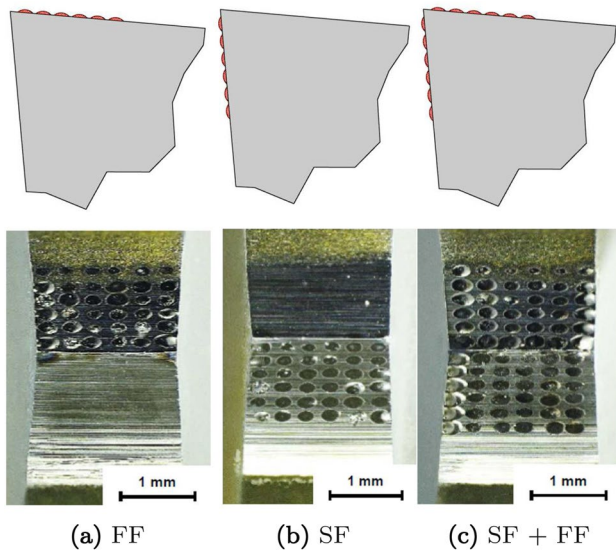


Fig. 5 Three variants of laser implanted tools used for orthogonal cutting tests. FF: Flank face implantation; SF: Rake face implantation; SF+FF: Rake + flank face implantation

row of implants (closest to the main cutting edge) being at a distance of 100 μm from the edge.

The workpiece material for the cutting tests was a spheroidal graphite cast iron EN-GJS-800-2. The material contains spheroidal shaped graphite inside ferritic zones in a pearlite matrix; a tensile strength of 800 MPa, an elongation at failure of 2% and Rockwell hardness of 38 HRc. The inherent lubrication property (due to graphite) of the material helps to avoid built-up edge (BuE) during dry cutting. Cutting tests were performed on a linear cutting rig designed to simulate the cutting action of a bandsaw with a single tooth (see Fig. 6). Forces in three directions were measured using Kistler 9257b dynamometer. For the determination of the cutting parameters, cutting tests with non-implanted (ground) tool were performed with the goal of minimizing the BuE. Based on these tests, a cutting speed (v_c) of 50 m/min and tooth feed (f_z) of 0.02 mm was selected for further tests.

The cutting tests were performed in two stages. First, cutting tests were performed with the four tool variations i.e. the non-implanted tool and the three variations of laser implanted tools shown in Fig. 5 to determine the variant producing greatest reduction in process forces compared to variant 1 (non-implanted tool). For this purpose, two 2 mm deep grooves with three samples of each variant were cut into the workpiece plate representing 200 cuts each being 300 mm long and having approximately 3 snds of non-cutting motion between each cut or 60 m total length of cut. In the second part of the cutting tests, longer experiments were performed with the selected variant of the implanted tool and the non-implanted tool to assess the effect of PLI on the tool life. For the comparison of tool wear between the non-implanted and implanted tools, three wear forms were measured namely the nose radius, wear of the main flank face and side flank. Wear limit for the tool life was set as 0.2 mm for flank wear land. Wear on the tool was measured under Leica Z16 microscope after every 1000 cutting cycles representing a cut surface area of 60 cm². Three repetitions were performed for each of the variants in both first and second phase of the cutting tests.

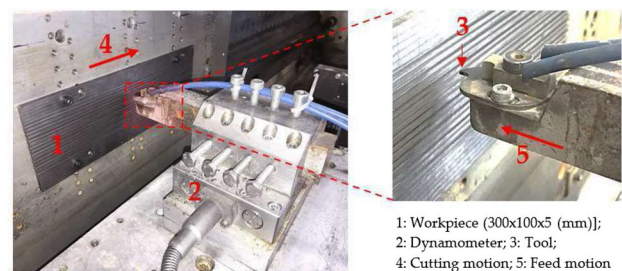


Fig. 6 Test apparatus for orthogonal cutting tests

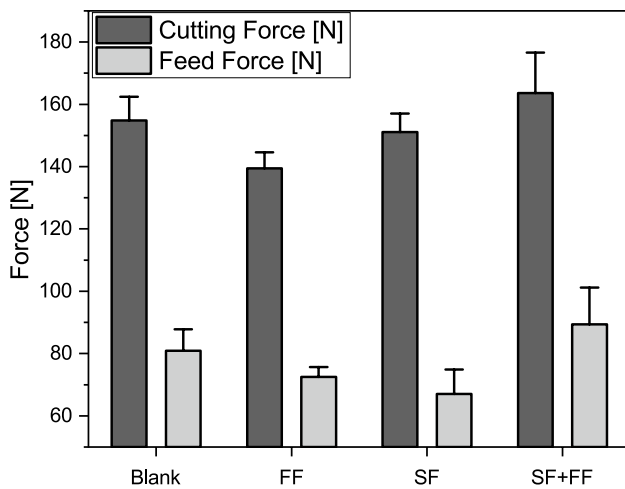


Fig. 7 Average of three ($N = 3$) cutting experiments for each of the four tool variations during the first 60 m length of cut

3 Results and discussion

Figure 7 shows the average cutting and feed forces from 200 cuts (amounting to a total length of cut $L = 60$ m) made with three samples of each of the four tool variants. The effect of tool wear for the first 60 m of cut is negligible (around $10 \mu\text{m}$) as seen in the plot of flank wear land width (V_b) against length of cut in Fig. 12. Compared to the non-textured tool (blank), the rake face (SF) implantation resulted in an average reduction of feed force by 17 % but only a 2 % reduction of cutting force. The variant with implants on both rake and flank faces (SF+FF) show increased values for feed force by 11 % and cutting force by 5 %. With only the flank surface implantation (FF) a reduction of 10 % of both feed and cutting forces was observed. The reduction in forces caused by flank face implantation were close to the 12 % reduction reported in [11] whereby flank face structuring with laser ablation was performed. Since cutting force constitutes the major portion of the total force, the tool variant causing the greatest reduction of cutting force, that is FF, was selected for wear analysis.

The reduction of cutting and feed forces with laser implanted tools in this study is in general less than that observed with laser ablated cutting tools (see Sect. 1.1). The laser implanted structures created here were limited to implanted spot diameters greater of around $200 \mu\text{m}$ due to the $88 \mu\text{m}$ spot diameter of the available laser. Thus the domes were in effect five times larger than the widths of the grooves created by various authors in literature by laser ablation texturing which had for example groove width and groove depths of $20 \mu\text{m}$ and $10 \mu\text{m}$ [22], $50 \mu\text{m}$ and $20 \mu\text{m}$ [11] and $2.2 \mu\text{m}$ and $1.3 \mu\text{m}$ [21]. The relatively larger textures obtained with PLI process could cause reduction of the shear angle or hinder the flow of the chip

as it would flow into the spaces between the individual implants as shown in the finite element analysis study conducted by Wu et al. [33]. The reduction of cutting force results from the reduction of tool/chip and tool/workpiece contact area resulting in lower resistance to chip flow and tool movement in the cutting direction. Therefore, a smaller sized texture on the rake face could lead to further reduction of cutting forces as the chip would glide over the implants without flowing into the spaces in between adjacent domes (see Fig. 8). Smaller textures will lead to greater surface area of contact between the tool and the chip and would lead to increased friction. However, the contact surface area will still be much smaller than that for non-implanted tool. The resistance to the flow of the chip will also be much smaller than that for the rake face with large implanted spots as the chip will not be able to flow between the adjacent implants.

3.1 Tool life analysis

Cutting tests with blank tools and implanted flank face tools were carried out for a total of 4000 cutting cycles representing a total length of cut of 1200 m. The tool life criteria was set either at doubling of the initial cutting or feed force or $200 \mu\text{m}$ average flank wear land. Figure 9 shows the force measurements of three samples of both tool types. The flank face modified tools did not show significant increase of the cutting and feed forces whereas the forces for the blank tool rose exponentially after about 400 m length of cut. This is primarily caused by the increase of the cutting edge radius which causes the tool to plough the workpiece instead of cutting it (see Sect. 3.2.3). For the implanted tools, the three test samples did not reach $200 \mu\text{m}$ flank wear and the tests were stopped after 1200 m length of cut. Thus the flank face implanted tool have caused improvement of the tool life by factor 3. In comparison, the published studies with laser ablated surface texturing of cutting tools have shown tool life improvements of 40–70% [1], 18% [11] and 10–30% [37].

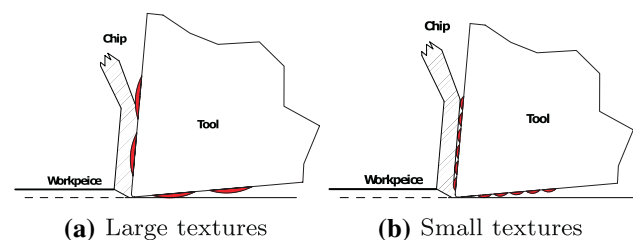
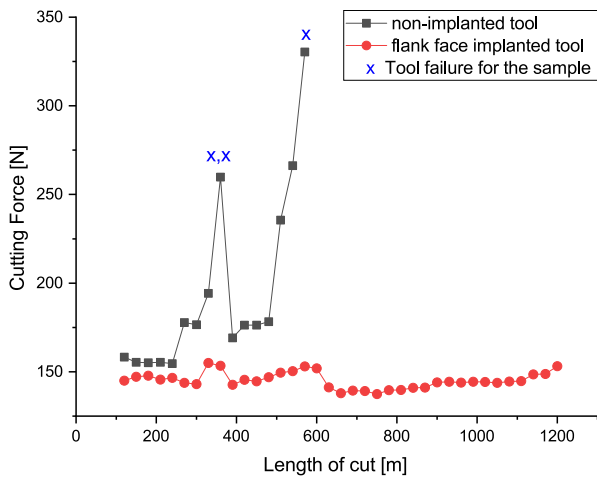
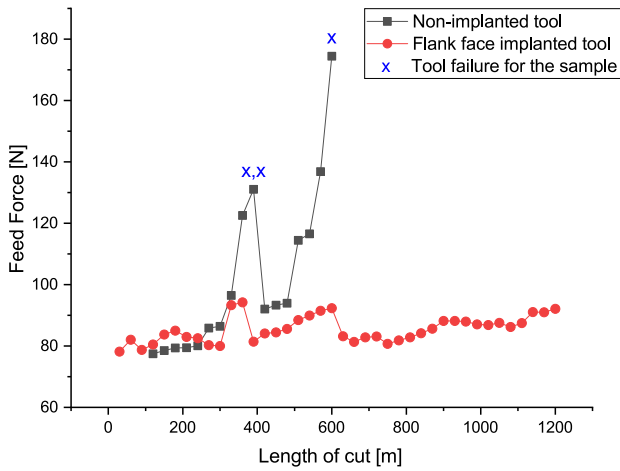


Fig. 8 Depiction of chip flow over the implanted textures on the rake face of the tool



(a) Cutting force



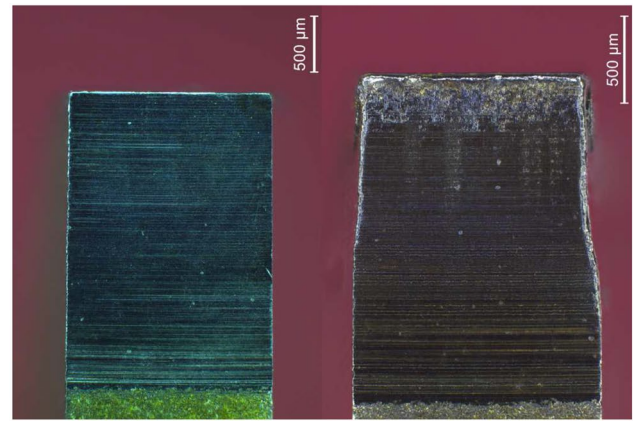
(b) Feed force

Fig. 9 Average cutting and feed force of three samples each of non-implanted and flank face implanted tools

3.2 Tool wear analysis

3.2.1 Side flank wear

The wear of the side flank faces shows a clear difference between the implanted and non-implanted cutting tools. The width of the non-implanted specimen reduced by approximately 220 μm (average value of three specimen) after 400 m of cutting length after which two of the three samples failed. The implanted cutting edges showed a tool width reduction of only 5.4 μm after a cutting length of 1200 m. Figure 10 shows one of the three specimens of both implanted and blank tools before and at the end of the cutting experiments.



(a) Non-implanted tool before (left) and after (right) 400 m length of cut



(b) Flank face implanted tool before (left) and after (right) 1200 m length of cut

Fig. 10 Wear of the side flank faces measured on the rake face

3.2.2 Main flank wear

To measure the wear land width (V_B), five measurements per cutting edge were made between the respective V_B and the original cutting edge using a light microscope and the average plotted over the cutting length as shown in Fig. 11. Graphically, a significantly stronger increase of the V_B is shown for the non-textured tools compared to the implanted tools. The non-textured tools showed a wear mark width of approx. 120 μm after a cutting length of 400 m, whereas the implanted tools showed wear mark widths of approx. 50 μm after a cutting length of 1200 m.

The results showed that for the first 400 m of cut the implanted tools result in approximately 80% reduction of flank wear compared to the non-textured tools. This is at least five times more than the 13% reduction reported in [10] for cutting AISI 4140 steel and four times more than the 21% reduction reported in [30] for turning Inconel 718

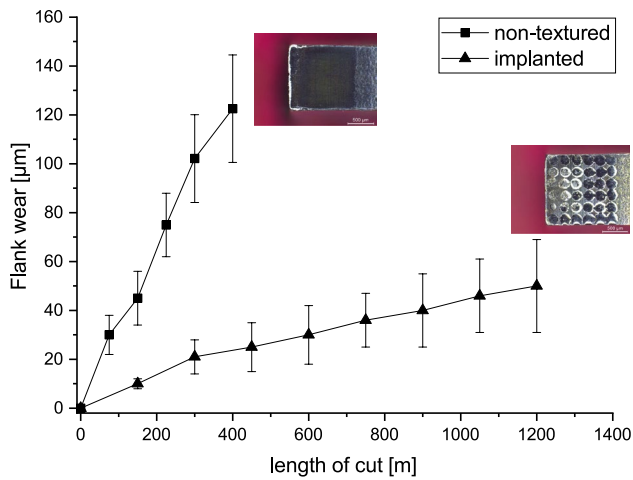


Fig. 11 Wear on the flank face for non-textured and implanted tools. (N=3)

alloy using subtractive (laser ablated) surface textures on cutting tools.

Figure 12 shows the 3d topography of one of the three samples each of worn non-textured and implanted tools. In particular, severe flank wear is visible through the greenish coloring on the non-implanted tool. On the implanted tools, it can be seen that the implants have experienced severe abrasive wear. Especially in the middle, near the cutting edge, there are hardly any elevations of the implants left intact. The relatively good condition of the domes at the

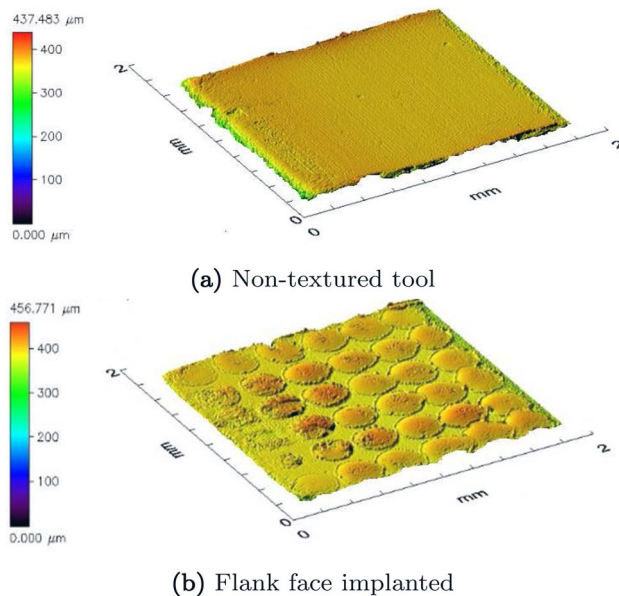


Fig. 12 3D topography of flank face of non-textured and implanted tools at the end of the cutting tests

lateral cutting edge corners and contours shows that implants have blocked the side flank wear from advancing further.

3.2.3 Cutting edge radius

The cutting edge radius was measured using the GFM MikroCAD light scanning microscope. For each measurement, 100 profile measurements per cutting edge were placed over the entire width of the edge. The edge radius of the tools in the ground state (start of the cutting tests) was 10 μm . Figure 13 shows the increase of edge radius for implanted and blank tools. The non-implanted tools show a sharp increase of the edge radius to over 20 μm in less than 200 m of cut resulting in the edge radius becoming larger than the uncut chip thickness or tooth feed resulting in ploughing instead of chip formation. The hard implantations seem to hinder the increment of the edge radius and result in only a 15 μm increase after 1200 m cut length.

4 Conclusions

Additive surface textures (micro-domes) were created on high speed steel tools using pulsed laser implantation of tungsten carbide particles. Dry cutting tests were performed on ductile cast iron EN-GJS-800-2 using the linear cutting test rig. The main conclusions were:

1. For the selected texture size the implantation of flank face has shown 10 % reduction of cutting force compared to only a 2 % reduction caused by rake face implantation.
2. Improvement of tool life by at least factor 3 was observed with flank face implanted tools compared to non-structured tools.

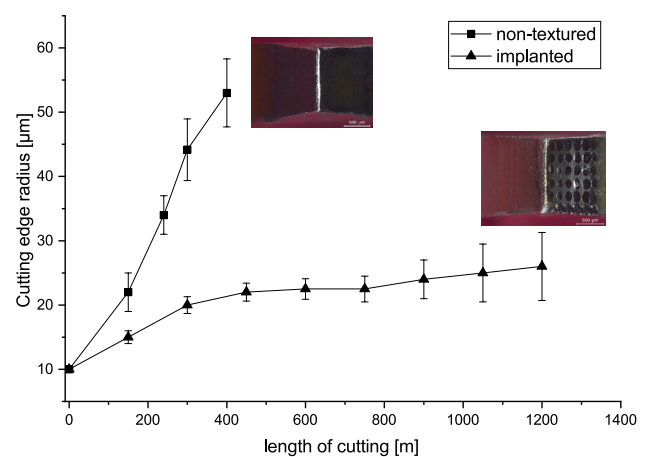


Fig. 13 Wear on the flank face for non-textured and implanted tools (N = 3)

3. Approximately 80% reduction of average width of flank wear land as well as 60% reduction of cutting edge blunting compared to non-textured tools was observed.
4. Implantation of the flank face significantly reduced the wear of side flank face from 12.9% reduction of edge width with non-textured tools after 400 m of cutting to only 0.3% with implanted tools after 1200 m.
5. Further research needs to be conducted in order to evaluate the effects of smaller implant size, other hard particles as well as the effect of laser implantation on cutting temperature, workpiece roughness, tool/chip contact, shear angle and coefficient of friction.

Funding Open Access funding enabled and organized by Projekt DEAL.

Compliance with ethical standards

Conflict of interest The authors declare that they have no conflict of interest.

Open Access This article is licensed under a Creative Commons Attribution 4.0 International License, which permits use, sharing, adaptation, distribution and reproduction in any medium or format, as long as you give appropriate credit to the original author(s) and the source, provide a link to the Creative Commons licence, and indicate if changes were made. The images or other third party material in this article are included in the article's Creative Commons licence, unless indicated otherwise in a credit line to the material. If material is not included in the article's Creative Commons licence and your intended use is not permitted by statutory regulation or exceeds the permitted use, you will need to obtain permission directly from the copyright holder. To view a copy of this licence, visit <http://creativecommons.org/licenses/by/4.0/>.

References

1. Ahmed YS, Paiva JM, Arif A, Amorim FL, Torres RD, Veldhuis SC (2020) The effect of laser micro-scale textured tools on the tool-chip interface performance and surface integrity during austenitic stainless-steel turning. *Appl Surf Sci* 510:145455. <https://doi.org/10.1016/j.apsusc.2020.145455>
2. Bailey JA (1975) Friction in metal machining—mechanical aspects. *Wear* 31(2):243–275. [https://doi.org/10.1016/0043-1648\(75\)90161-1](https://doi.org/10.1016/0043-1648(75)90161-1)
3. Braham-Bouchnak T, Germain G, Morel A, Furet B (2015) Influence of high-pressure coolant assistance on the machinability of the titanium alloy ti555-3. *Mach Sci Technol* 19(1):134–151. <https://doi.org/10.1080/10910344.2014.991029>
4. Childs T (2006) Friction modelling in metal cutting. *Wear* 260(3):310–318. <https://doi.org/10.1016/j.wear.2005.01.052>
5. Ciftci I (2006) Machining of austenitic stainless steels using cvd multi-layer coated cemented carbide tools. *Tribol Int* 39(6):565–569. <https://doi.org/10.1016/j.triboint.2005.05.005>
6. Denkena B, Grove T, Krödel A, Ellersiek L (2018) Increased performance in high speed turning of inconel 718 by laser structuring of pcbn tools. *Procedia CIRP* 77:602–605. <https://doi.org/10.1016/j.procir.2018.08.202>
7. Enomoto T, Sugihara T (2010) Improving anti-adhesive properties of cutting tool surfaces by nano-/micro-textures. *CIRP Ann* 59(1):597–600. <https://doi.org/10.1016/j.cirp.2010.03.130>
8. Enomoto T, Sugihara T, Yukinaga S, Hirose K, Satake U (2012) Highly wear-resistant cutting tools with textured surfaces in steel cutting. *CIRP Ann* 61(1):571–574. <https://doi.org/10.1016/j.cirp.2012.03.123>
9. Evans CJ, Bryan JB (1999) “structured”, “textured” or “engineered” surfaces. *CIRP Ann* 48(2):541–556. [https://doi.org/10.1016/s0007-8506\(07\)63233-8](https://doi.org/10.1016/s0007-8506(07)63233-8)
10. Fatima A, Mativenga PT (2015) A comparative study on cutting performance of rake-flank face structured cutting tool in orthogonal cutting of aisi/sae 4140. *Int J Adv Manufact Technol* 78(9–12):2097–2106. <https://doi.org/10.1007/s00170-015-6799-6>
11. Fatima A, Mativenga PT (2016) Performance of flank face structured cutting tools in machining of aisi/sae 4140 over a range of cutting speeds. *Proc Inst Mech Eng Part B: J Eng Manuf* 230(1):3–18. <https://doi.org/10.1177/0954405414555589>
12. Fox V, Jones A, Renevier N, Teer D (2000) Hard lubricating coatings for cutting and forming tools and mechanical components. *Surf Coat Technol* 125(1–3):347–353. [https://doi.org/10.1016/S0257-8972\(99\)00611-8](https://doi.org/10.1016/S0257-8972(99)00611-8)
13. Fukui H, Okida J, Omori N, Moriguchi H, Tsuda K (2004) Cutting performance of dlc coated tools in dry machining aluminum alloys. *Surf Coat Technol* 187(1):70–76. <https://doi.org/10.1016/j.surfcoat.2004.01.014>
14. Gachot C, Rosenkranz A, Hsu SM, Costa HL (2017) A critical assessment of surface texturing for friction and wear improvement. *Wear* 372–373:21–41. <https://doi.org/10.1016/j.wear.2016.11.020>
15. Hilgenberg K (2014) Investigation of the self-organising behaviour of laser implanted tool surfaces. *Berichte zur Metallformgebung, vol, vol 5*. Kassel University Press, Kassel
16. Hilgenberg K, Behler K, Steinhoff K (2014) Localized dispersing of ceramic particles in tool steel surfaces by pulsed laser radiation. *Appl Surf Sci* 305:575–580. <https://doi.org/10.1016/j.apsusc.2014.03.137>
17. Hilgenberg K, Rethmeier M, Steinhoff K (2016) Surface structuring by pulsed laser implantation. *Mater Sci Forum* 879:750–755. <https://doi.org/10.4028/www.scientific.net/MSF.879.750>
18. Hügel H, Graf T (2009) *Laser in der Fertigung*. Vieweg+Teubner, Wiesbaden, <https://doi.org/10.1007/978-3-8348-9570-7>
19. Jesudass Thomas S, Kalaichelvan K (2018) Comparative study of the effect of surface texturing on cutting tool in dry cutting. *Mater Manuf Processes* 33(6):683–694. <https://doi.org/10.1080/10426914.2017.1376070>
20. Kathrein M, Michotte C, Penoy M, Polcik P, Mitterer C (2005) Multifunctional multi-component pvd coatings for cutting tools. *Surf Coat Technol* 200(5–6):1867–1871. <https://doi.org/10.1016/j.surfcoat.2005.08.105>
21. Kawasegi N, Sugimori H, Morimoto H, Morita N, Hori I (2009) Development of cutting tools with microscale and nanoscale textures to improve frictional behavior. *Precision Eng* 33(3):248–254. <https://doi.org/10.1016/j.precisioneng.2008.07.005>
22. Kiyota H, Itoigawa F, Nakamura T (2014) Experimental research of micro-textured tool for reduction in cutting force. *Key Eng Mater* 611–612:1258–1263. <https://doi.org/10.4028/www.scientific.net/KEM.611-612.1258>
23. Kustas FM, Fehrehnbacher LL, Komanduri R (1997) Nanocoatings on cutting tools for dry machining. *CIRP Ann* 46(1):39–42. [https://doi.org/10.1016/s0007-8506\(07\)60771-9](https://doi.org/10.1016/s0007-8506(07)60771-9)
24. Li Q, Pan C, Jiao Y, Hu K (2019) Investigation on cutting performance of micro-textured cutting tools. *Micromachines*. <https://doi.org/10.3390/mi10060352>
25. Schüddekopf S, Mienert G, Weidig U, Böhm S (2018) Standzeitverlängerung von rührreißschweißwerkzeugen durch den einatz

- von laserstrahlimplantaten. extension of the service life of friction stir welding tools through the use of laser beam implants. *Schweissen und Schneiden* 70(9):642–649
26. Schuleit N, Fletcher D, Steinhoff K, Kapoor A (2000) Improvement of mechanical and tribological properties of forming tools by 3d thermal implants with dispersed metal carbide particles. In: *Proceedings of 4th European Mechanics Conference*, Metz, 2000, EDP Sciences
 27. Spranger F, Hilgenberg K (2019) Laser implantation: an innovative technique for surface texturing. *PhotonicsViews* 16(1):38–41. <https://doi.org/10.1002/phvs.201900002>
 28. Steinhoff K, Schuleit N, Fletcher D, Kapoor A (2000) Thermal implantation of metal carbide particles: A new surface treatment for cold forging tools. In: *10th International cold forging congress*, Stuttgart-Fellbach, Germany, 13-15 Sep. 2000, VDI Berichte, VDI Verlag, pp 243–260
 29. Sun J, Wong YS, Rahman M, Wang ZG, Neo KS, Tan CH, Onozuka H (2006) Effects of coolant supply methods and cutting conditions on tool life in end milling titanium alloy. *Mach Sci Technol* 10(3):355–370. <https://doi.org/10.1080/10910340600902181>
 30. Tamil AN, Zeman P, Hoier P, Beno T, Klement U (2019) Investigation of micro-textured cutting tools used for face turning of alloy 718 with high-pressure cooling. *J Manuf Process* 37:606–616. <https://doi.org/10.1016/j.jmapro.2018.12.023>
 31. Tanabe I, Hoshino H (2018) Development of a new forced cooling technology using a high-pressure coolant for machining difficult-to-machine materials. *Journal of Manufacturing and Materials Processing* 2(2):39. <https://doi.org/10.3390/jmmp2020039>
 32. Universität Kassel, Institut für Produktionstechnik und Logistik Fachgebiet Trennende und Fügende Fertigungsverfahren (????) Abschlussbericht - gradierte oberflächen durch laserbearbeitung für rührreißschweißwerkzeuge erhöhter standzeit: Igf-nr.: 18.841 n (dvs-nr.: 05.064)
 33. Wu Z, Bao H, Liu L, Xing Y, Huang P, Zhao G (2020) Numerical investigation of the performance of micro-textured cutting tools in cutting of ti-6al-4v alloys. *Int J Adv Manuf Technol*. <https://doi.org/10.1007/s00170-020-05428-1>
 34. Xing Y, Deng J, Zhao J, Zhang G, Zhang K (2014) Cutting performance and wear mechanism of nanoscale and microscale textured al2o3/tic ceramic tools in dry cutting of hardened steel. *Int J Refract Metal Hard Mater* 43:46–58. <https://doi.org/10.1016/j.ijrmhm.2013.10.019>
 35. Yamaguchi K, Takada Y, Tsukuda Y, Ota M, Egashira K, Morita T (2016) Friction characteristics of textured surface created by electrical discharge machining under lubrication. *Procedia CIRP* 42:662–667. <https://doi.org/10.1016/j.procir.2016.02.298>
 36. Yan P, Rong Y, Wang G (2016) The effect of cutting fluids applied in metal cutting process. *Proc Inst Mech Eng Part B: J Eng Manuf* 230(1):19–37. <https://doi.org/10.1177/0954405415590993>
 37. Ze W, Jianxin D, Yang C, Youqiang X, Jun Z (2012) Performance of the self-lubricating textured tools in dry cutting of ti-6al-4v. *Int J Adv Manuf Technol* 62(9–12):943–951. <https://doi.org/10.1007/s00170-011-3853-x>

Publisher's Note Springer Nature remains neutral with regard to jurisdictional claims in published maps and institutional affiliations.